Available online at www.sciencedirect.com

ScienceDirect

Energy Procedia 129 (2017) 248–255

Energy Procedia

www.elsevier.com/locate/procedia

IV International Seminar on ORC Power Systems, ORC2017
13-15 September 2017, Milano, Italy

Real Gas Expansion with Dynamic Mesh in Common Positive Displacement Machines

Nicola Casari*,[a], Alessio Suman[a], Mirko Morini[b], Michele Pinelli[a]

[a] *University of Ferrara, via Saragat 1, 44121 Ferrara, ITALY*
[b] *University of Parma, Department of Engineering and Architecture, Parco Area delle Scienze 181/a, 43124 Parma, ITALY*

Abstract

Fluids processed by the machinery involved in ORC cycles undergo several transformations among which the expansion in positive displacement machines. The fluid path inside this component is very complicated and gaps play a crucial role. Due to the importance of this technical detail, gap design and optimization is a decisive step in achieving an high efficiency both of the expander and the whole cycle. In this work the fluid dynamics of several fluids commonly used in ORC cycles is investigated. Particularly, their behaviour during the expansion through the gap in operation is numerically investigated. The effects of the gap formation and its evolution on the processed fluid is studied thanks to a dynamic mesh approach. A typical application has been considered in this work: the variable gap between the fixed and mobile spirals of a scroll expander is analysed.

The relative motion and in turn, the variation of the gaps during the machine operation, implies the use of particular numerical strategies able to well represent these localized geometrical features. On the top of that, the modelling of the processed fluids as a real gas determines an extra effort in the way of representing the actual behavior involved in the positive displacement machine operation. This analysis shows the local fluid dynamic phenomena due to the variable clearances. R134a and its replacements R152a and R1234ze(E), fluids widespread in the ORC cycles, are used in this work. The fluids are investigated under the same conditions and effects like separation and shock wave are highlighted.

This analysis allows the comprehension of how local phenomena could affect the overall machine operation and efficiency. Gaps are the responsible of the volumetric efficiency of the machine and, coupled with (i) time-variable geometry modification, (ii) relative velocities and (iii) fluid characteristics characterize the global ORC system performance.

Keywords: Scroll; Single Screw; Variable Gap Analysis; Real Gas expansion; CFD;

* Corresponding author. Tel.: +39 0532 974964
E-mail address: nicola.casari@unife.it

1876-6102 © 2017 The Authors. Published by Elsevier Ltd.
Peer-review under responsibility of the scientific committee of the IV International Seminar on ORC Power Systems.
10.1016/j.egypro.2017.09.150

1. Introduction

The performance of the ORC system should be optimized by choosing the right expander geometry and operating conditions [1]. In fact, for micro-ORC applications, the issues related to the components usually involve expander and pump efficiency. This piece of information can be easily gathered by considering the number of prototype systems [2]. Positive displacement machines are widely use in ORC systems as expanders replacing turbogenerators for micro-ORC applications [3]. Indeed turbines see dramatic efficiency losses when the enthalpy jump is low or the conditions at which energy is available are unsteady [4].

The complexity of the expander design is further amplified by the non-ideal thermo-physical behavior of organic fluids in the conditions of interest. In some cases expansion process could take place in proximity to the saturated vapor curve or close to the critical point. Severe real gas effects arise and complex multi-parameter equations of state are necessary for a proper representation of the actual phenomena by means of analytical model or more in general, by fluid dynamic calculations [3].

Positive displacement machine performances are heavily influenced by the sealing systems between the stationary and moving parts. In light of this, understanding the local flow phenomena can help improving the design. Since a precise and detailed experimental campaign is very challenging, the Computational Fluid Dynamics (CFD) can help in such a task. Several examples of the numerical simulation of this kind of component can be found in [5–8]. Two are the main challenges involved in the CFD analysis: the rotor motion and the properties of the refrigerant. The complexity of the domain-motion simulation brought about the rise of several numerical strategies, whereas real gas effects for refrigerants are numerically modelled in order account for the modification of the shock structures and of the flow field [9–11]. With regards to the relation between volumetric expanders and real gas behavior, the real gas model implies differences in the power output calculation [12] or, more in general, in the correct representation of the gas expansion [13].

In this paper, a detailed CFD analysis is realized related to the gas expansion phenomena involved in a scroll expander [7]. Three different fluids commonly employed in the ORC systems (i.e. R134a, R152a and R1234ze(E)) have been analyzed and their behaviour was compared with the air considered as a real gas. The geometry investigated in this work is representative of the flank gap of a scroll expander. A 2D transient analysis have been carried out, following the rotation of the machine for an angle of 150°. This angular rotation have been chosen for numerical reasons: beyond this threshold the mesh quality degenerates in the set-up proposed in this work. In order not to map the solution on another mesh, to avoid interpolation errors, the comparison among the fluids have been done within this angle. The full 360° investigation would be indeed helpful both in the design phase as well as in the analysis. If the entire revolution is investigated, the actual interaction between the dynamic effects due to the displacement of the moving spiral and the time evolution of the gap could be studied. Eventually a law of variation of the gap size over the evolution of the expander motion might be derived in order to optimize the geometry of this geometric feature.

The analysis in this work, carried out with the open-source software OpenFOAM-v1606+, will particularly focus upon the fluid dynamics of the flow downstream the gap, and the determination of how different fluids behave within the analysed gap. These details are of paramount importance for the optimization of the design rather than the setting of lumped parameters model.

Nomenclature

C_d Coefficient of discharge
R Gas constant

Greek symbols
γ Specific heat ratio

Subscripts
0 Inlet / Total quantities
e Outlet quantities

2. Methodology

In this work the application of CFD to a scroll expander is proposed. For the purpose of this analysis, that is the investigation of the behaviour of the flow through the flank gap of the machine, the axial gap will not be considered. Therefore a 2D analysis will be performed, assuming as representative of the machine the mid section of the spiral height. The study will follow the domain in its evolution in order to catch the behaviour of the fluid expanding through the gap during the rotation of the shaft.

2.1. Geometry and Mesh

The overall geometry and the position of the domain here analyzed are reported in Fig. 1

The study is performed on a structured mesh. The sensitivity to the grid size have been carried out spanning from 1500 to 6500 elements in order to better represent the phenomenon. An example of the mesh used for the simulation of the phenomenon is reported in the section 3. With such a setup, the y+ averaged both over time and over space is equal to 70 for the inner (moving) spiral and 150 for the outer (fixed) spiral.

2.2. Fluids Investigated and Real Gas Model

The machinery presented in 2.1 was numerically simulated with different fluids. Basically the family of fluids comprehensive of the R134a and its replacements R152a [14] and R1234ze(E) [15] have been investigated. Relevant chemical properties and environmental information of these alternative refrigerants are reported in Tab. 1.

As one can see from Tab. 1, the three refrigerants have comparable pressure and temperature at the critical point and, being the GWP decreasing from R134a to the R1234ze(E) the last one is considered the replacement for the first one. The Ozone Depletion Potential (ODP), not reported in Tab. 1, is equal to 0 for all the considered fluids. In order to model the fluid behaviour inside the machinery, the variation of the thermophysical quantities as a function of the temperature must be declared. Commonly, in CFD software, there are several ways available to supply the

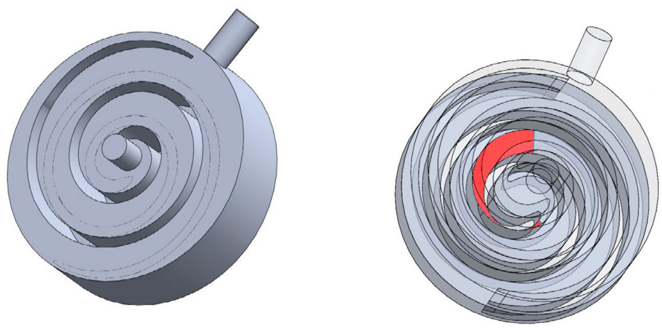

(a) Overall geometry of the scroll expander (b) Particular analyzed (in red)

Fig. 1: Overall geometry of the machine and position of the domain analyzed

Table 1: Chemical and environmental properties of R134a, R152a and R1234ze(E)

Fluid	Chemical Formula	Molar Mass [kg/kmol]	Global Warming Potential [GWP]	Critical Pressure [MPa]	Critical Temperature [K]	Critical Density [kg/m^3]	Acentric Factor [-]
R134a	$C_2F_4H_2$	102	1430	4.06	374.2	511.9	0.327
R152a	$C_2F_2H_4$	66	140	4.52	386.4	368.0	0.275
R1234ze(E)	$C_3F_4H_2$	114	4	3.64	382.5	489.2	0.313

desired function of variation of such quantities. In this work the change of the transport quantities (viscosity μ and conductivity κ) as well as the specific heat c_p are supplied via polynomial correlations. The NIST data have been used in order to get the value at constant pressure equal to 1 MPa. It has been verified that at the lowest and highest pressure within the flow field, the deviation from the value predicted with the implemented polynomials is below the 5%.

Among the quantities derived by polynomial interpolation of the Helmholtz equation (NIST database), it is worthy to report here the viscosity variation with the temperature. In Fig. 2, the trend of the viscosity with the temperature is reported. It can be see that the viscosity of the R152a is remarkably lower than R134a in same conditions. This fact will of course reflects on a very different behaviour downstream the gap. Evidences of this remark are reported in section 3.

For what concerns the equation of state for the gas with real gas behaviour the model presented in this work implements a form of the semi-empirical van der Waals equation of state. Such an equation was proposed by van der Waals as a modification of the ideal gas law, in order to take into account the size of the molecules and the molecular interaction force [16]. Particularly, the Peng-Robinson model is employed here [17]. This model requires the properties of the fluid at the critical point and the acentric factor ω, reported in Tab. 1. This is because at the critical point the first and the second derivatives of the pressure with respect to the volume vanish [17] and thus the EOS can be solved. The acentric factor was proposed as a measure of the amount by which the properties of a substance differ from those predicted by the principle of corresponding states [18].

2.3. Numerical model

The numerical simulation carried out employs a compressible solver together with a dynamic mesh motion solver for the displacement of the grid points. Details regarding the numerical solver employed (i.e. *rhoPimpleDyMFoam*), a solver that combines the PISO and SIMPLE algorithm, can be found in [19] and in [20] the dynamic mesh solver is described.

In this work three fluids are analysed: R134a, R152a and R1234ze(E). Being the last two candidate for replacing the first one, the conditions used in this numerical investigation are the same. In all the cases, the inlet (total) pressure is equal to 1.1 MPa. The inlet total temperature is set equal to 390 K. The numerical method employed is implicit, nonetheless a maximum Courant number equal to one is imposed, for accuracy reasons. This led to a maximum time step of roughly 1 μs. The total amount of iterations per time step is such that the residuals descend below 10^{-4} up to a maximum of 150. A total time of 0.0133 s is simulated. For what concerns the turbulent model, a standard k-ε model has been applied. The boundary conditions at the inlet are based on the mixing length (assumed equal to 0.0002 m) and at the walls standard wall functions have been applied.

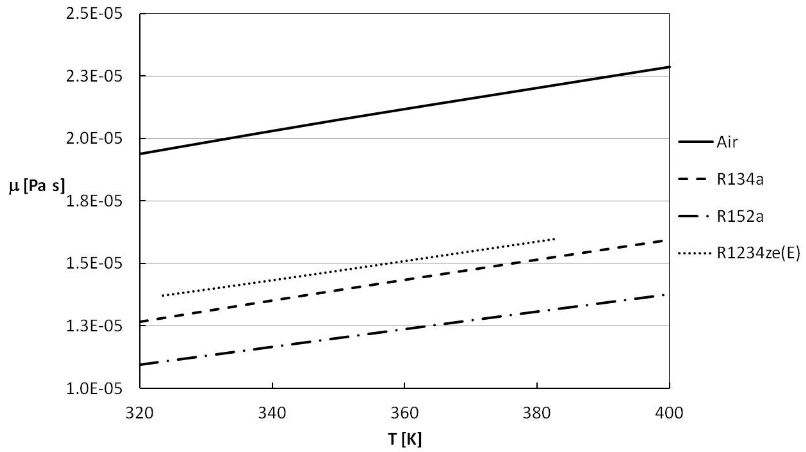

Fig. 2: Variation of the viscosity with the temperature for the 4 fluids analysed

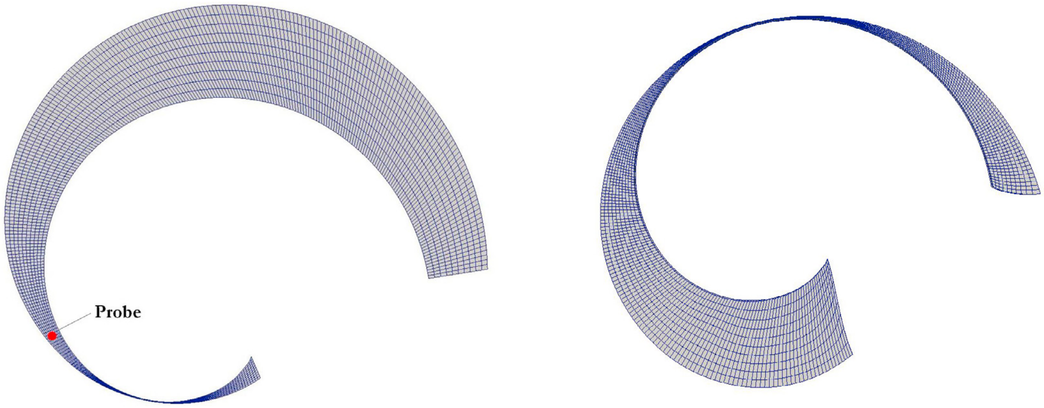

(a) Scroll Mesh at 0° and probe position (b) Scroll Mesh at 150°

Fig. 3: Evolution of the orbit over the first 150° of shaft rotation

3. Results

The evolution of the orbit have been analysed over the first 150° of shaft rotation. The extreme conditions are reported in fig. 3. The pressure jump has been imposed across the gap. Assuming for the R134a a constant specific heat ratio γ equal to 1.135 [21], the critical pressure ratio (i.e. the pressure ratio under which the nozzle is chocked) is equal to 0.577. An inlet total pressure of 11 bar would require thus an outlet pressure of 6.35 bar in order the nozzle to be chocked. Since the outer pressure imposed in this analysis is 6 bar, the flow should become supersonic downstream the throat.

In the following the behaviour of all the fluids will be compared from the overall gap performance point of view. Then the detailed comparison between the fluid currently employed in the machine (i.e. R134 a) and the most recent replacement (i.e. R1234ze(E)) will be carried out.

The variation of the static pressure during the evolution of the rotation as measured by a numerical probe is reported in fig. 4. The probe is held fixed in the gap wile the inner spiral of the scroll evolves and its position is reported in fig. 3a. This is the same values one would get back-tracking a fluid particle in its trajectory. Starting from 0° the probe is downwind with respect to the gap and thus register instabilities in pressure given by the transient shedding downwind the obstacle. Then the pressure falls sharply (in what is a sharp rise in the flow direction). This represent a shock wave due to a pressure ratio higher than the critical ratio. The pressure is recovered as the inner spiral passes by, to reach a plateau corresponding to the inlet pressure. The trend does not register ripples in this area (on the contrary with respect to downwind the gap) since no obstacle to the fluid flow is present.

A very interesting comparison can be carried out if one investigates the mass flow rate that manages to make its way through the gap. In fig. 5 the variation of the mass flow rate with the revolution of the crank angle Θ is reported. It can be seen that all the fluids have roughly the same trend, but the R134a and the R1234ze(E) show a mass flow rate which is almost twice the one of the R152a. On the same graph the variation of the throat section is reported. It can be seen that, in the range of crank angle investigated, the minimum distance passes from 7 x 10^{-6} m to above 100 x 10^{-6}. The flow rate trend is closely related to the one of the area, even if dynamic effects justify the deflections from the pure geometric variation of the passage area.

The perhaps intuitive behaviour one can expect from the viscosity differences, i.e. fig. 2, is confirmed by fig. 6. The volume flow rate is plotted in this case and it can be seen that the R152a has the highest volume flow rate. The remarkable difference with the mass flow rates of fig. 5 is due to the fact that the R152a has a density which is roughly one half of the other two fluids investigated. On the top of that the relative position of R134a and R1234ze(E) in this graph seems to confirm a sort of opposite trend with the viscosity.

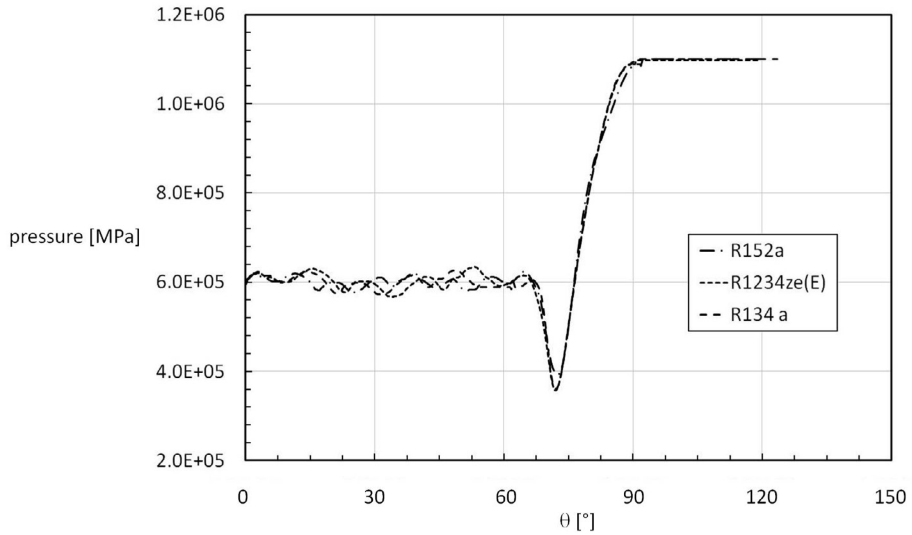

Fig. 4: Variation of the pressure in a fixed point as the shaft angle Θ increases

The behaviour of the flow downstream the gap, described in figure 4 is confirmed by the density contour reported in fig. 7. The shock wave downstream the nozzle is the only way the R134a has, as any other fluid, for recovering pressure, since the back pressure is above the isentropic value.

It must be remarked that such shock waves are not stable structures since the unsteadiness of the scroll motion is such that separations behind the gap arise. Thus complicate shock boundary layer interactions form raising the complexity of this kind of analyses. The highly unsteadiness of the phenomenon is also proved by the evolution of the flow field reported in fig. 8. As one can see from fig. 8(b) the assumption of steady flow downstream the gap over the crank-angle evolution does not hold here. One must expect a coefficient of discharge variable with the evolution of the motion.

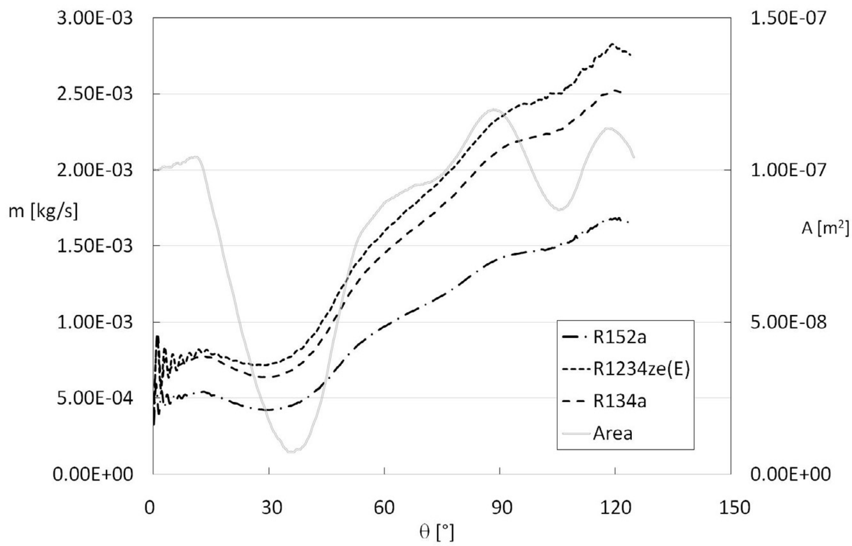

Fig. 5: Mass flow rate and throat area variation along the evolution of the crank angle. Area to be read on the right axis

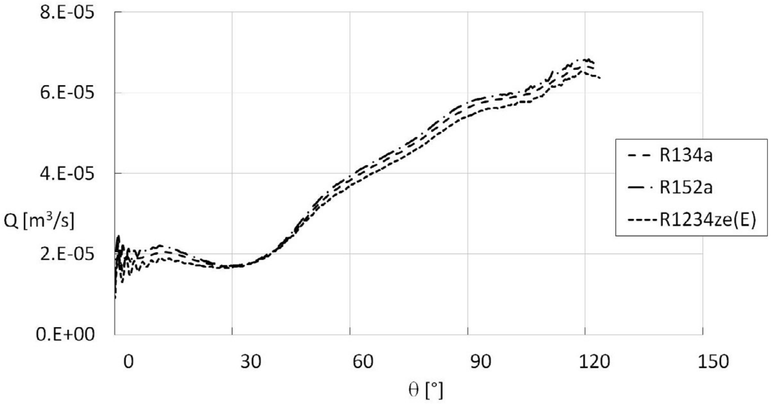

Fig. 6: Volumetric flow rate and throat area variation along the evolution of the crank angle

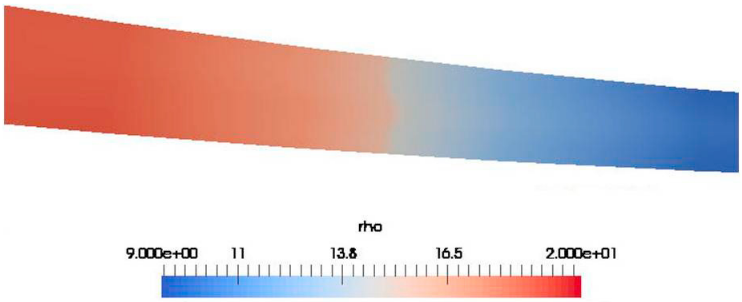

Fig. 7: Density variation across the shock downstream the gap for R134a

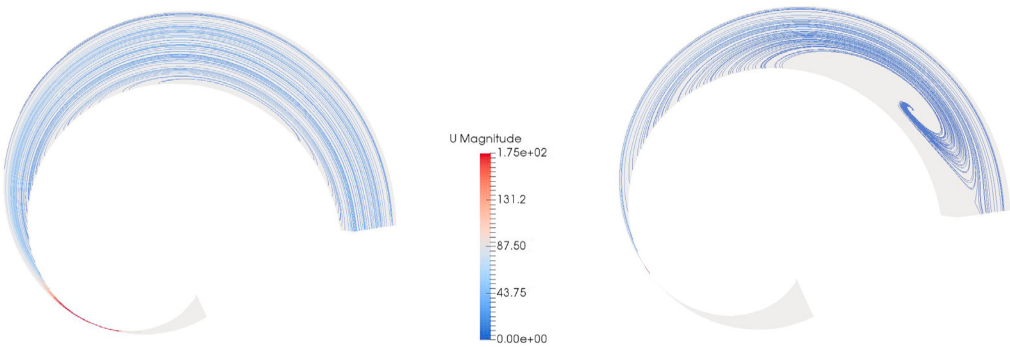

(a) Flow field at position 0°

(b) Flow field at position 30°

Fig. 8: Evolution of the Flow field: streamlines and particular of separation of R134a due to the curvature of the duct.

4. Conclusion

In this work the numerical analysis of a positive displacement machines commonly employed in ORC cycles have been carried out. Particularly, the gaps area have been studied deeply. The approaches used involve both a dynamic mesh analysis and the modelling of the working fluid as real gas. The expansion through the typical clearances of a scroll expander was analyzed. Three different fluids have been investigated and the corresponding performance of the gap are reported.

It can be seen that the leakage flow has an inverse behaviour with respect of the viscosity if the volumetric flow rate through the gap is kept into account. The great differences in the density forbid a generalization of this statement to the mass flow rate, where the opposite results have been obtained.

The present analysis shows how inadequate steady analyses of the clearance could be, since the wall displacement is not taken into account. The unsteadiness of the flow field due to the moving wall is indeed remarkable and can influence the flow rate through the gap entailing a reduced passage area downwind the gap, and provoking a decrease in the coefficient of discharge.

References

[1] Vincent Lemort, Ludovic Guillaume, Arnaud Legros, Sébastien Declaye, and Sylvain Quoilin. A comparison of piston, screw and scroll expanders for small scale rankine cycle systems. In *Proceedings of the 3rd International Conference on Microgeneration and Related Technologies*, 2013.

[2] Arnaud Landellea, Nicolas Tauverona, Philippe Haberschillc, Rémi Revellinc, and Stephane Colassona. Performance evaluation and comparison of experimental organic rankine cycle prototypes from published data. 2016.

[3] Astolfi M. Macchi E. *Organic Rankine Cycle (ORC) Power Systems, Technologies and Applications*, volume 107. Duxford: Woodhead Publishing Series in Energy, 2016.

[4] Gianluca Montenegro, Augusto Della Torre, Angelo Onorati, Dalia Broggi, Gerd Schlager, and Christian Benatzky. Cfd simulation of a sliding vane expander operating inside a small scale orc for low temperature waste heat recovery. Technical report, SAE Technical Paper, 2014.

[5] Ahmed Kovacevic, Nikola Stosic, and Ian Smith. *Screw Compressors: Three Dimensional Computational Fluid Dynamics and Solid Fluid Interaction*, volume 46. Springer Science & Business Media, 2007.

[6] Alessio Suman, Davide Ziviani, Jacopo Gabrielloni, Michele Pinelli, Michel De Paepe, and Martijn Van Den Broek. Different numerical approaches for the analysis of a single screw expander. *Energy Procedia*, 101:750–757, 2016.

[7] Mirko Morini, Claudio Pavan, Michele Pinelli, Eva Romito, and Alessio Suman. Analysis of a scroll machine for micro orc applications by means of a re/cfd methodology. *Applied Thermal Engineering*, 80:132–140, 2015.

[8] Jen-Chieh Chang, Chao-Wei Chang, Tzu-Chen Hung, Jaw-Ren Lin, and Kuo-Chen Huang. Experimental study and cfd approach for scroll type expander used in low-temperature organic rankine cycle. *Applied Thermal Engineering*, 73(2):1444–1452, 2014.

[9] D Del Campo, R Castilla, GA Raush, PJ Gamez Montero, and E Codina. Numerical analysis of external gear pumps including cavitation. *Journal of fluids engineering*, 134(8):081105, 2012.

[10] Piero Colonna, John Harinck, Stefano Rebay, and Alberto Guardone. Real-gas effects in organic rankine cycle turbine nozzles. *Journal of Propulsion and Power*, 24(2):282–294, 2008.

[11] John Harinck, Teemu Turunen-Saaresti, Piero Colonna, Stefano Rebay, and Jos van Buijtenen. Computational study of a high-expansion ratio radial organic rankine cycle turbine stator. *Journal of Engineering for Gas Turbines and Power*, 132(5):054501, 2010.

[12] Iva Papes, Joris Degroote, and Jan Vierendeels. New insights in twin screw expander performance for small scale orc systems from 3d cfd analysis. *Applied Thermal Engineering*, 91:535–546, 2015.

[13] JM Luján, JR Serrano, V Dolz, and J Sanchez. Model of the expansion process for r245fa in an organic rankine cycle (orc). *Applied Thermal Engineering*, 40:248–257, 2012.

[14] Jitendra Kumar Verma, Ankit Satsangi, and Vishal Chaturani. A review of alternative to r134a (ch3ch2f) refrigerant. *International Journal of Emerging Technology and Advanced Engineering, ISSN*, pages 2250–2459, 2013.

[15] Radhouane Ben Jemaa, Rami Mansouri, Ismail Boukholda, and Ahmed Bellagi. Energy and exergy investigation of {R1234ze} as {R134a} replacement in vapor compression chillers. *International Journal of Hydrogen Energy*, pages –, 2016.

[16] Paul M Fishbane, Stephen G Gasiorowicz, and Stephen T Thornton. *Physics*. Prentice-Hall, 2005.

[17] Ding-Yu Peng and Donald B Robinson. A new two-constant equation of state. *Ind. Eng. Chem. Fundam*, 15(1):59–64, 1976.

[18] K E Betts, JS Rowlinson, and G. Saville. *Thermodynamics for chemical engineer*. The MIT Press, Cambridge, Massachusetts, 1975.

[19] Esteban Gonzalez. Cfd simulations of acoustic and thermoacoustic phenomena in internal flows. In *46th AIAA Fluid Dynamics Conference*, page 3960, 2016.

[20] Hrvoje Jasak and Zeljko Tukovic. Automatic mesh motion for the unstructured finite volume method. *Transactions of FAMENA*, 30(2):1–20, 2006.

[21] Dupont. Thermodynamic properties of HFC 134a. Technical report.